Laser ablation of Silicon for the Buried Contact Solar Cells application

Vansh Tibrewal[1]

[1]*Dhirubhai Ambani International School, Mumbai, Maharashtra, India*

---***---

Abstract - *Creating grooves to make the metal buried is one of the important steps in the production of a buried contact solar cell. Various techniques are used to ablate the material such as photolithography, diamond scratching, chemical etching, and laser ablation. Laser ablation is an ultra-fast, easy, and reliable method to ablate material from a silicon wafer. Thus, in the present study, I have developed a one-dimensional laser heating model of the nanosecond laser to predict the temperature profile. Further, the effects of different laser parameters such as the average laser power, repetition rate of the pulse, and width of the pulse are also observed on the temperature generated during the laser matter interaction. From the study it is found that the surface temperature increases with power, whereas with increase in pulse width and pulse repetition rate, the surface temperature decreases. Furthermore, with an 80% decrease in power, a 70% reduction in surface temperature is observed and with an 80% reduction in pulse width, a 30% increase in surface temperature is observed. A 30% increase in the repetition rate of the pulse leads to the surface temperature being halved. These indicates that laser power has the highest influence on surface temperature followed by pulse repetition rate and pulse width.*

***Key Words*: Nanosecond laser**, **Buried contact solar cell**, **Laser ablation**, **response surface methodology**, **temperature profile**

1.INTRODUCTION

Due to increasing demand for energy, power generation using non-conventional energy resources is becoming popular day by day. In this study, the role of laser ablation in the fabrication of the buried contact silicon based solar cell is explored. This technology eliminates screen-printed contacts with 25% better performance. The metal (copper) is filled (buried) in the laser ablated region in the silicon substrate, which allows high aspect ratio. The buried metal releases freer electron than the substrate silicon while interacting with photon from the incident solar light. This allows closely spaced metal fingers with high transparency. In standard silicon based solar cells, the shading loss is around 10 to 13%, whereas in the case of buried contact solar cell, the shading loss is only around 2 to 2.5%. This ultimately leads to improvement in the performance of the solar cell.

Grooving in the buried contact solar cell can be formed in several ways including plasma etching, mechanical scribing, ion beam machining, photolithography, laser ablation, or laser grooving, and wafer saw grooving. Laser cutting has several advantages compared to mechanical cutting or alternate cutting processes. During laser cutting, there is no direct contact with the material, and thus the contaminants cannot be embedded into the material, and the material remains pure. Laser cutting produces a high-quality, complex cut and can be used to cut several parts simultaneously. It does this clean cutting while having a minimal heat-affected zone.

Various researchers have made efforts to develop models to ablate silicon using a laser. Fell et al. [1] have developed numerical model-based enthalpy for continuous laser radiation. They have evaluated the shape of the groove and experimental validation was also performed to calculate the model accuracy. Parandoush and Hossain [2] have used CO_2 and Nd:YAG millisecond lasers for various applications such as grooving and cutting. They have solved 2D heat conduction equation and evaluated the temperature profile in the domain. Furthermore, they have considered the effect of scanning speed on kerf width.

Response surface methodology is an efficient method to understand the effect of individual parameters along with the interaction [3]. Lee at al. [4] developed 3D finite element model and predicted the ablation process. During the study they have used response surface methodology and design of experiments [5]. In the literature, a detailed parametric study of laser ablation has not been performed through simulation.

In the present work, a one-dimensional (1D) laser heating model is developed for nanosecond laser with gaussian profile. Moreover, the effect of laser parameters like pulse repetition rate, pulse width and average laser power on temperature profile and ablation profile is predicted along with the thermal damage. Further, to try to understand the interactions between the various laser parameters, response surface methodology is used to design a set of process parameters. The code to simulate the temperature variation is developed in Python.

2. SIMULATION APPROACH

2.1 Problem definition

When the laser beam is moved on top of the silicon surface, it interacts with the material and heat and plasma are generated, as a result of which grooves are formed with a certain depth and width. The heat is transferred in both directions, transverse and longitudinal. The temperature gradient in the longitudinal direction is very high compared to that in the transverse direction. Therefore, it is possible to

assume the problem is one-dimensional rather than two-dimensional to avoid complexity.

A computational model was built for studying the temperature profile and depth of ablation for different laser parameters. The problem can be seen in Figure 1. We have assumed the heat transfer in one dimension only i.e. the x-direction and also that the there is no heat transfer to the surrounding from top and bottom surfaces because the outside medium is taken as vacuum.
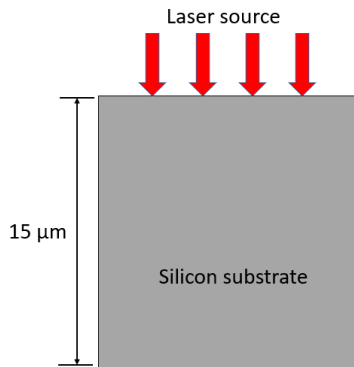

Figure 1 Model description

2.2 Laser matter interaction

Laser matter interaction consists of heat transfer due to conduction inside the material. So, we begin with the governing equation (Fourier heat conduction) for one-dimensional heat transfer which is given by [6],

$$\frac{\partial H}{\partial t} = \frac{\partial}{\partial x}\left(K\frac{\partial Q}{\partial x}\right) + Q_{source}$$

Assuming material properties to be constant we get,

$$\rho C_p \frac{\partial T}{\partial t} = K\frac{\partial^2 Q}{\partial x^2} + Q_{source}$$

where, ρ is the density, C_p is the specific heat, K is thermal conductivity, T is the temperature, t is time, x is coordinate in x-direction and Q_{source} is the laser heat source which is being applied as an external energy source and it is given by [7],

$$Q_{source} = \alpha I(x)$$

$$= \alpha I_l \exp(-\alpha x)$$

$$= \alpha(1-R)I_0 \exp(-\alpha x)$$

Equation 4 is Beer Lambert's law, where α is the absorption coefficient, I_L is the laser intensity, I_0 is laser intensity at the surface and R is the reflectivity.

The reflectivity is given by the Fresnel Equations [8] i.e.

$$R = \left(\frac{\widetilde{n_1} - \widetilde{n_2}}{\widetilde{n_1} + \widetilde{n_2}}\right)^2$$

$$\tilde{n} = n + ik$$

where, n is the refractive index and k is the extinction coefficient for a particular material and wavelength. The numbers 1 and 2 in the subscript corresponds to the two mediums (Figure 2).

$$R = \frac{(n_1 - n_2)^2 + (k_1 - k_2)^2}{(n_1 + n_2)^2 + (k_1 + k_2)^2}$$

and the absorption coefficient is given by,

$$\alpha = \frac{4\pi k_2}{\lambda}$$

where λ is the wavelength of beam.

Hence the final equation for the laser heating in the body can be formulated as

$$\frac{\partial T}{\partial t} = \frac{K}{\rho C_p}\frac{\partial^2 Q}{\partial x^2} + \frac{\alpha(1-R)I_0\exp(-\alpha x)}{\rho C_p}$$
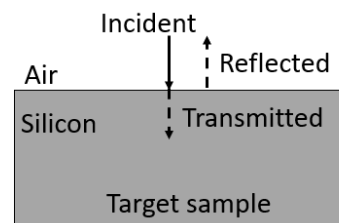

Figure 2 Transmission and reflectance

2.3 Response Surface Methodology (RSM)

In the present study we have considered three parameters (refer table 1) with five levels and a total of fifteen experiments were designed as shown in table 2.

Table 1 Parameters with levels

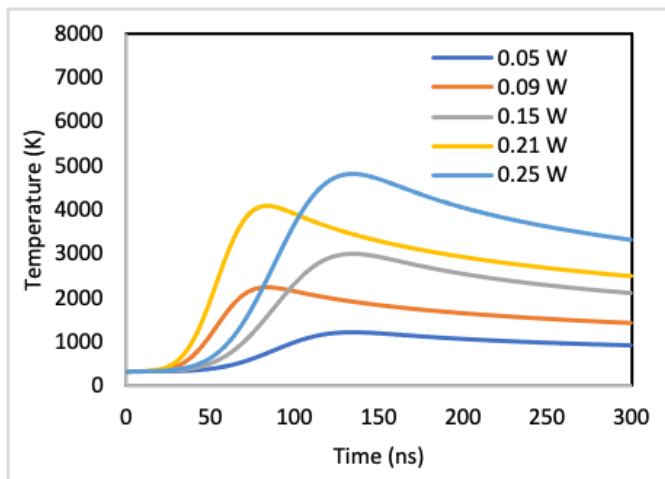| Level and Parameters	-2	-1	0	1	2
Frequency (KHz)	30	32	35	38	40
Power (W)	0.05	0.09	0.15	0.21	0.25
Pulse width (ns)	20	36	60	84	100

Figure 3 Variation in temperature with time at different value of power

Table 2 set of process parameters

Sr. No	PRR (KHz)	Power(W)	Pulse width (ns)
1	32	0.09	36
2	38	0.09	36
3	32	0.21	36
4	38	0.21	36
5	32	0.09	84
6	38	0.09	84
7	32	0.21	84
8	38	0.21	84
9	30	0.15	60
10	40	0.15	60
11	35	0.05	60
12	35	0.25	60
13	35	0.15	20
14	35	0.15	100
15	35	0.15	60

.

3. RESULTS AND DISCUSSION

In this section the simulation has been conducted and using that the evolution of the temperature profile has been discussed

3.1 Effect of laser power

In Figure 3 variation in temperature with time is shown at different values of laser power. During "pulse on" time, temperature increases and once "pulse on" time is over, temperature starts falling exponentially. Furthermore, it is observed that as power increases, maximum temperature increases. As laser power increases, intensity increases, which results in high heat input and leads to high temperature generation [9].

The temperature variation along the depth is shown in Figure 4 at different values of average laser power. The maximum temperature is observed at the surface, and it decreases exponentially along the depth. Maximum and minimum surface temperature is observed for 0.25 W and 0.05 W power respectively. When power is decreased by 80%, a 70% reduction in surface temperature is observed.
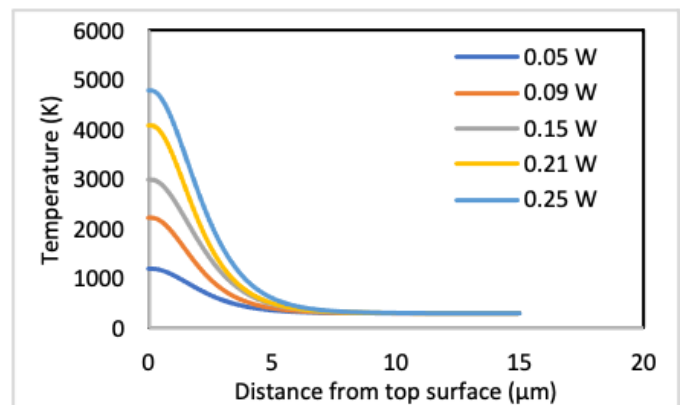

Figure 4 Variation in temperature along the depth at different value of power

3.2 Effect of pulse repetition rate

In Figure 5, temperature variation with time at different values of pulse repetition rate is shown. With an increase in pulse repetition rate maximum temperature decreases. This could be because an increase in pulse repetition rate leads to a decrease in heat input per unit area which leads to reduction in heat generation [10]. The maximum temperature was observed at a pulse repetition rate of 30 kHz.
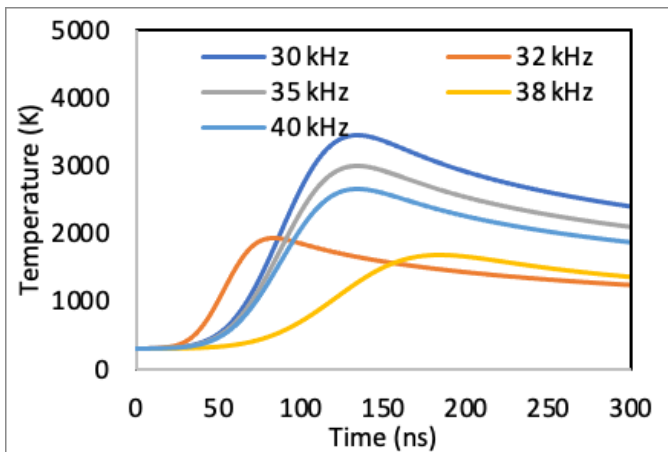
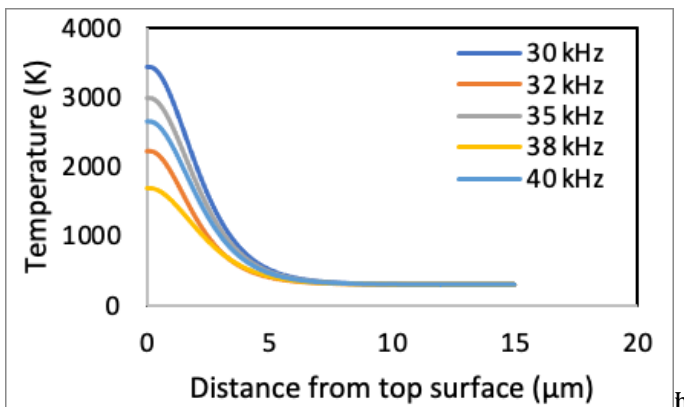Figure 5 Variation in temperature with time at different value of pulse duration

Figure 6 Variation in temperature along the depth at different value of pulse repetition rate

Figure 6, variation in temperature along the depth is shown at different values of pulse repetition rate. Temperature is observed to be maximum at the surface and reduces along the depth. With a 33% increase in pulse repetition rate, around 50% decrease in surface temperature is observed.

3.3 Effect of pulse duration

In Figure 7, variation in temperature with time is shown at different values of pulse width. The maximum temperature is observed at the lowest pulse width of 20 nanosecond, and temperature is decreasing continuously with an increase in pulse duration. With an increase in pulse width, heat energy is distributed over a longer period of time which allows material to dissipate heat.

In Figure 8, variation in temperature along the depth is shown at different values of pulse width. With an 80% decrease in pulse width, there is a 30% increase in the surface temperature.
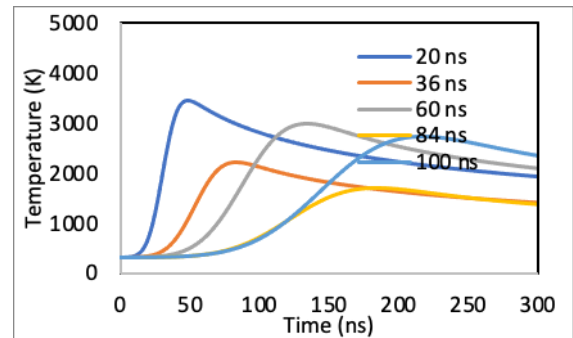

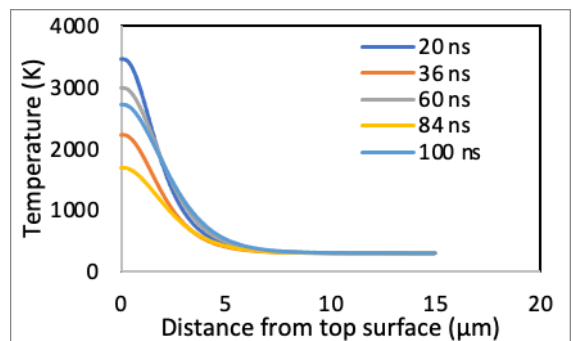Figure 7 Variation in temperature with time at different value of pulse width

Figure 8 Variation in temperature along the depth at different value of pulse width

4. CONCLUSIONS

In the present work, a 1D laser heating model is developed to simulate the temperature variation in the silicon wafer. The effect of various laser parameters on temperature is also capture using the generated model. Following are the important conclusions drawn from the present study:

1. With a decrease in average power, maximum surface temperature decreases. In contrast, surface temperature is observed to increase with a decrease in pulse width.
2. With an 80% decrease in power, there is a 70% reduction in surface temperature.
3. A 30% increase in repetition rate of the pulse causes a 50% reduction in the surface temperature.
4. With an 80% decrease in pulse width, a 30% increase in surface temperature is observed.

REFERENCES

[1] A Fell, D Kray, and GP Willeke. Transient 3d/2d simulation of laser-induced ablation of silicon. Applied Physics A, 92(4):987{991, 2008.

[2] P Parandoush and A Hossain. A review of modeling and simulation of laser beam machining. International journal of machine tools and manufacture, 85:135{ 145, 2014.

[3] Gunst, R. F., 1996, "Response Surface Methodology: Process and Product Optimization
Using Designed Experiments," Technometrics, 38(3), pp. 284–286.

[4] Lee J, Yoo J, Lee K. Numerical simulation of the nano-second pulsed laser ablation process based on the finite element thermal analysis. Journal of Mechanical Science and Technology. 2014 May 1;28(5):1797-802.

[5] Rana, Pinal, Divyanshu Bhartiya, Meinam Annebushan Singh, and Deepak Marla. "Multi-Objective Optimization of Wire Electrical Discharge Machined Ultra-Thin Silicon Wafers Using Response Surface Methodology for Solar Cell Applications." In International Manufacturing Science and Engineering Conference, vol. 84263, p. V002T08A021. American Society of Mechanical Engineers, 2020.

[6] H. Lim and J. Yoo, FEM based simulation of the pulsed laser ablation process in nanosecond fields, Journal of Mechanical Science and Technology, 25 (7) (2011) 1811-1816.

[7] J. T. Houghton, The Physics of atmospheres 2nd edition, Cambridge University Press, Cambridge, United Kingdom (2002).

[8] Yevick D, Friese T, Schmidt F. A comparison of transparent boundary conditions for the Fresnel equation. Journal of Computational Physics. 2001 Apr 10;168(2):433-44.

[9] Gerhards M. High energy and narrow bandwidth mid IR nanosecond laser system. Optics communications. 2004 Nov 16;241(4-6):493-7.

[10] Hamamatsu Photonics KK, Shimo-Kanzo I. Thermo-Elastic-Plastic Analysis on Internal Processing Phenomena of Single-Crystal Silicon by Nanosecond Laser.